THE JOURNAL OF PHYSICAL CHEMISTRY B

ARTICLE

pubs.acs.org/JPCB

New Insight in Protein−Ligand Interactions. 2. Stability and Properties of Two Mutant Forms of the D-Galactose/D-Glucose-Binding Protein from *E. coli*

Olga V. Stepanenko,[†] Alexander V. Fonin,[†] Olesya V. Stepanenko,[†] Kateryna S. Morozova,[‡] Vladislav V. Verkhusha,[‡] Irina M. Kuznetsova,[†] Konstantin K. Turoverov,[*,†] Maria Staiano,[§] and Sabato D'Auria[*,§]

[†]Laboratory of Protein structure, stability and folding of proteins, Institute of Cytology RAS, 194064 St. Petersburg, Russia

[‡]Department of Anatomy and Structural Biology, Albert Einstein College of Medicine, Bronx, New York, United States

[§]Laboratory for Molecular Sensing, IBP-CNR, 111 80131 Naples, Italy

ABSTRACT: The galactose/glucose-binding protein from *E. coli* (GGBP) is a 32 kDa protein possessing the typical two-domains structure of the ligand-binding proteins family. GGBP is characterized by low dissociation constant values with respect to glucose binding, displaying an affinity constant for glucose in micromolar range. This feature makes GGBP unsuitable as a sensitive probe for continuous glucose monitoring in blood of diabetic patients. In this work we designed, produced, and characterized two mutant forms of GGBP carrying the following amino acid substitutions in the active center of the protein: W183A or F16A. The two mutant GGBP forms retained a globular structure similar to that of the wild-type GGBP and displayed an affinity for glucose lower than the wild-type GGBP. A deep inspection of the entire set of the obtained results pointed out that the N- and C-terminal domains of GGBP-W183A in the absence of glucose have a stability lower than that of the wild-type protein. In the presence of glucose, the two domains of GGBP-W183A were tightly bound, making the protein structure more stable to the action of denaturing agents. On the contrary, the mutant form GGBP-F16A possesses a very restricted structural stability both in the absence and in the presence of glucose. In this work the role of Phe 16 and W 183 are discussed with regard to the structural and functional features of GGBP. In addition, some general guidelines are reported for the design of a novel glucose biosensor based on the use of GGBP.

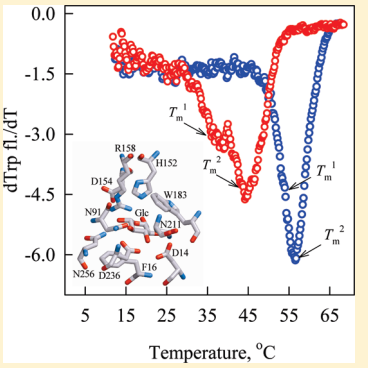

INTRODUCTION

Millions of people are affected by diabetes mellitus. Prolonged excessive blood sugar levels in patients with diabetes can lead to the development of blindness, nephritic insufficiency, diseases of the cardiovascular and nervous system, and the occurrence of inborn defects.[1,2] Frequent and life long control of blood sugar levels is required to prevent dangerous consequences of this disease. Monitoring of blood glucose is also necessary to avoid the excessive consumption of medication and, the risk of insulin shock, which can lead to coma and even death.[3,4]

The general method for measuring blood sugar in diabetic patients is regular blood sampling from the finger of the patient.[5] This procedure is painful, and the majority of patients try to reduce the number of the blood samplings. Thus development of noninvasive methods for continuous glucose monitoring would be highly desirable. However, the problem of creating commercially favorable and minimally or noninvasive devices for accurate persistent glucose monitoring that are comparable with the currently available invasive methods has not yet been solved.[6−8] An analysis of sugar concentrations in humans can be performed by glucose measurements not only from blood, but also from intercellular liquids, tears, urine, oral and optical mucous membranes, cornea, and ear-drums.[1,4]

One of the most promising directions for persistent glucose monitoring is the design and development of biosensor systems in which glucose specifically binds to proteins acting as the sensitive element. The D-galactose/D-glucose-binding protein (GGBP) from *E. coli* appears to be a good candidate for such a sensitive element as the interaction between GGBP and glucose results in a substantial conformational reorganization of the tertiary structure of the protein.[8,9] GGBP belongs to a class of the periplasmic ligand-binding proteins which activate the high-affinity transport of a large number of compounds (for example, carbohydrates, amino acids, anions, metal ions, dipeptides and oligo-peptides), promote chemo-taxis toward different substances, and are in some cases involved in bacteria quorum sensing.[10,11] The GGBP is 32 kDa protein having the typical two-domains structure of ligand-binding proteins.[12,13] Both the N-terminal and the C-terminal domains of the protein consist of six β-sheets framed by two or three α-helices.[12,14] Located in a deep cleft between the two domains, the ligand-binding site of GGBP is composed of a set of amino acids which include the

Received: May 16, 2011
Revised: June 10, 2011
Published: June 14, 2011

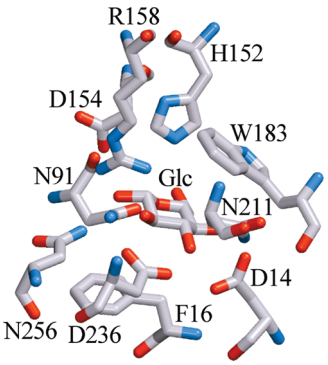

Figure 1. Structure of ligand-binding site of GGBP. It is shown the localization of Phe 16 and Trp 183 residues which sandwich the glucose molecule in an aromatic pocket. Eight polar amino acids distributed between N- and C-terminal domains of protein form a strong network of hydrogen bonds with all of the hydroxyls and oxygen atoms of the glucose ring. Carbon, nitrogen, and oxygen are gray, blue, and red, respectively. The figure has been created on the basis of PDB[48] data with the file 2GBP.ent[13] using the graphical software VMD[49] and Raster 3D.[50]

aromatic residues Trp 183 and Phe 16 (Figure 1). These residues sandwich the glucose molecule in an aromatic pocket and play a significant role for the binding of ligands.[12,13,15]

Wild-type GGBP is characterized by low dissociation constant values (1 μM) of the protein/glucose complex[13,16] with respect to the glucose concentrations encountered in the human blood. This characteristic of the protein makes wild-type GGBP not useful as a sensitive probe for the design of a continuous glucose monitoring biosensor in the blood of diabetic patients. To adjust the sensitivity of the biosensor system to the range of glucose concentrations present in the blood of healthy people (3−6 mM) or of diabetic patients (over 8 mM), it is necessary to change the GGBP dissociation constant to millimolar range.[17] The values of the GGBP dissociation constant could be modified by substituting either Trp183 or Phe16 that are located in the protein active center with nonaromatic residues. However, it is conceivable that these substitutions might affect not only the protein affinity for glucose but also its structure and stability.[18]

In this work, we have constructed GGBP mutant variants with either the W183A or the F16A substitution. Since Trp 183 and Phe 16 residues are directly involved in the protein function, we have addressed the question of whether or not these GGBP variants still possess the property of binding glucose. An important and desirable feature of biosensor system is its stability under different denaturing conditions. Thus, we have performed a comparative study of the structure and stability of the two GGBP variants both in the absence and in the presence of glucose.

MATERIALS AND METHODS

Plasmids, Mutagenesis, and Protein Expression. D-Glucose (Sigma, U.S.A.), guanidine hydrochloride (GdnHCl; Nacalai Tesque, Japan), and acrylamide (AppliChem, Germany) were used without additional purification. *E. coli* strain K-12 (F^+ *mgl503 lacZ lacY*$^+$ *recA1*) carrying an mglB gene deletion[16,19] transformed with a pTz18u-mglB vector was used. Upon induction with D-fructose,[20] the expression efficiency of the GGBP protein was rather low. The recombinant protein yield in this system does not exceed 5−8 mg/L of culture. Therefore, the mglB gene was recloned into a pET-11d plasmid with the T7 promoter (Stratagene, U.S.A.) using *NcoI* and

Forward primer:
5'- AG CC ***ATG*** GCT AAT AAG AAG GTG TTA ACC CTG TCT GCT GTG ATG G -3'

Reverse primer:
5'- AC AGA TCT TTA *ATG GTG ATG GTG ATG GTG* gcc tcc gcc TTT CTT GCT GAA TTC AGC CAG G -3'

Figure 2. Sequences of specific forward and reverse primers for GGBP. New restriction sites for NcoI (CCATGG) and *Bgl*II (AGATCT) are shown in gray. The underlined codon of forward primer has been added to create the restriction site for NcoI. The stop-codon is written in white letters on a black background. The translation initiation site is marked in bold italic. The sequences encoding the polyhistidine tag at the C-terminal of the protein and the linker are indicated in italic and lower case characters, respectively.

*Bgl*II restriction sites. Specific forward and reverse primers (sequences are indicated in Figure 2) were used to insert new restriction sites and a poly histidine tag at the C-terminal of the gene. Site-directed mutagenesis was performed with the Quik-Change mutagenesis kit (Stratagene, U.S.A.) using primers encoding corresponding to amino acid substitutions. Plasmids were isolated from bacterial cells using plasmid DNA isolation kits (Omnix, Russia). Primer purification was performed using either reverse-phase chromatography or electrophoresis in a polyacrylamide gel.

pET-11d plasmids encoding for wild-type GGBP (GGBPwt) and GGBP-F16A and GGBP-W183A mutants were used to transform *E. coli* BL21(DE3) cells. The expression of the proteins was then induced by adding 0.5 mM isopropyl-beta-D-1-thiogalactopyranoside (IPTG; Nacalai Tesque, Japan). Bacterial cells were cultured for 24 h at 37 °C. Recombinant proteins were purified using Ni^+-agarose packed in His-GraviTrap columns (GE Healthcare, U.S.A.). Protein purification was controlled using denaturing SDS-electrophoresis in 15% polyacrylamide gel.[21]

Concentrations of the protein samples were ranged from 0.2−0.7 mg/mL in all experiments. For the formation of the protein−ligand complex, 10−100 mM D-glucose was added to the protein solution. Measurements were performed in a 20 mM Na-phosphate buffer at pH 8.0.

Fluorescence Spectroscopy. The fluorescence experiments were carried out using a Cary Eclipse spectrofluorimeter (Varian, Australia) with microcells (10 × 10 mm; Varian, Australia). Fluorescence anisotropy and fluorescence lifetime were measured using a homemade spectrofluorimeters with steady-state and time-resolved excitation[22] using microcells (101.016-QS 5 × 5 mm; Hellma, Germany). The excitation wavelengths for the fluorescence spectra were 297 and 280 nm. The spectral bandwidths of the fluorescence experiments were 2.5 nm. The position and form of the fluorescence spectra were characterized by the parameter $A = I_{320}/I_{365}$, where I_{320} and I_{365} are the fluorescence intensities measured at the emission wavelengths of 320 and 365 nm, respectively.[23] The values of parameter A and the fluorescence spectra were corrected using the instrument's spectral sensitivity. The contribution of tyrosine residues was characterized by the value $\Delta_{\lambda,\mathrm{Tyr}} = (I_\lambda/I_{365})_{280} - (I_\lambda/I_{365})_{297}$.

The equilibrium dependences of the different fluorescence characteristics of GGBPwt and its mutant variants on the GdnHCl concentration were recorded following incubation of the protein in solutions with the appropriate concentration of denaturant at 4 °C overnight. In the case of complex of GGBPwt with glucose the incubation time was prolonged to several days. The measurements were done at 23 °C. To determine the GdnHCl concentration, we relied on the measurement of the refraction coefficient using Abbe refractometer (LOMO, Russia).

Parametric Relationship between Two Independent Extensive Characteristics of the System for Protein Folding−Unfolding Studies. For a more detailed analysis of the protein unfolding process and in order to determine the number of intermediate states appearing on the pathway from the native protein state to the unfolded protein state, we used a parametric representation of the two independent extensive parameters of the system. Any extensive characteristic of a system consisting of two components is determined by the simple equation

$$I(\theta) = \alpha_1(\theta)I_1 + \alpha_2(\theta)I_2 \cdot \quad (1)$$

where I_1 and I_2 are the values of $I(\theta)$ at 100% content of the first and the second component, respectively, and $\alpha_1(\theta)$ and $\alpha_2(\theta)$ are the relative fraction of these components in the system, $\alpha_1(\theta) + \alpha_2(\theta) = 1$, where θ is any parameter depending of which the content of the components is changed. Denaturant concentration, temperature, pH of the solution, etc. can be taken as a parameter. Only for extensive characteristics which give quantitative characterization of the system, eq 1 is valid and the fraction of the components in the system, as well as the equilibrium constant K, can be determined by simple equations

$$\alpha_1(\theta) = \frac{I(\theta) - I_2}{I_1 - I_2}, \quad \alpha_2(\theta) = \frac{I_1 - I(\theta)}{I_1 - I_2},$$
$$K(\theta) = \frac{I_1 - I(\theta)}{I(\theta) - I_2} \quad (2)$$

If intensive characteristics (such as fluorescence spectrum position, parameter A, fluorescence anisotropy etc., which characterize the system qualitatively) are used these equations for determination of $\alpha_1(\theta)$, $\alpha_2(\theta)$, and $K(\theta)$ are not valid,[24] though often no account is taken of this in the investigations of protein conformation transition. For any two independent extensive characteristics, we have

$$I_1(\theta) = \alpha_1(\theta)I_{1,1} + \alpha_2(\theta)I_{2,1} \quad (3)$$

and

$$I_2(\theta) = \alpha_1(\theta)I_{1,2} + \alpha_2(\theta)I_{2,2} \quad (4)$$

Eliminating $\alpha_1(\theta)$ and $\alpha_2(\theta)$ from eqs 3 and 4, we can obtain the relationship between $I_1(\theta)$ and $I_2(\theta)$

$$I_1(\theta) = a + bI_2(\theta) \quad (5)$$

Equation 5 means that if with the change of parameter θ the transition between states 1 and 2 follows the model "all or none" without formation of the intermediate states, then the parametric relationship between any two extensive characteristics must be linear. If the experimentally recorded parametric relationship between two extensive characteristics of the system is not linear, it unequivocally means that the process of the transition from the initial to the final state is not a one-stage process but it proceeds with the formation of one or several intermediate states. This approach has been used for characterization of intermediate states of a number of proteins.[25−28]

Calculation of Protein Thermodynamic Characteristics. The equilibrium dependences of protein fluorescence intensity at the fixed registration wavelength upon GdnHCl concentration were used for the evaluation of free energy in native and unfolded states difference ΔG^0. The thermodynamic characteristics of protein stability were calculated according to the standard scheme[29]

$$I([D]) = \frac{I_N + I_U\, exp[-\Delta G^0([D])/RT]}{1 + exp[-\Delta G^0([D])/RT]} \quad (6)$$

The approximation of experimental data was performed via the nonlinear regression method using the Sigma Plot program.

Protein Affinity Measurements. The fluorescence intensity of protein solution in the ligand presence can be determined by a simple equation

$$I(C_0) = \alpha_F(C_0)I_F + \alpha_B(C_0)I_B \quad (7)$$

where I_F and I_B are the fluorescence intensity of protein in free state and bounded with ligand, respectively, and $\alpha_F(C_0)$ and $\alpha_F(C_0)$ are the relative fraction of this protein states in the solution at concentration of added ligand C_0, $\alpha_F(C_0) + \alpha_B(C_0) = 1$. Thus, the fraction of bounded protein is determined as

$$\alpha_B = \frac{I(C_0) - I_F}{I_B - I_F} = \frac{C_b}{C_p} \quad (8)$$

where C_p is the total protein concentration and C_b is the concentration of protein bounded with ligand.

The dissociation constant, K_d can be expressed as follows

$$K_d = \frac{[protein][ligand]}{[complex]} = \frac{(C_p - C_b)C_f}{C_b} \quad (9)$$

where C_f is concentration of free ligand, which can be calculated from the equation

$$C_b = C_0 - C_f \quad (10)$$

here C_0 is concentration of added ligand. Eliminating C_f from the eq 9, we can obtain the next equation for C_b

$$C_b = \frac{(K_d + C_p + C_0) - \sqrt{(K_d + C_p + C_0)^2 - 4C_pC_0}}{2} \quad (11)$$

Combining the eqs 8 and 11, we have the equation for definition of K_d, using the difference of fluorescence intensity of mutant proteins in the presence and in the absence of glucose. The wavelength of registration was chosen as that of the maximal difference in the fluorescence intensity of the ligand-free and bound states of the studied protein

$$I(C_0) = I_F + (I_B - I_F)\frac{(K_d + C_p + C_0) - \sqrt{(K_d + C_p + C_0)^2 - 4C_pC_0}}{2C_p} \quad (12)$$

Approximation of experimental data was performed via the nonlinear regression method using Sigma Plot program.

Circular Dichroism Measurements. CD spectra were obtained using a Jasco-810 spectropolarimeter (Jasco, Japan). Far-UV CD spectra were recorded in a 1 mm path length cell from 260 to 190 nm with a step size of 0.1 nm. Near-UV CD spectra were recorded in a 10 mm path length cell from 320 to 250 nm with a step size of 0.1 nm. For all spectra, an average of 3 scans was obtained. CD spectra of the appropriate buffer solution were recorded and subtracted from the protein spectra.

Stern−Volmer Quenching and Estimation of the Bimolecular Quenching Rates. To evaluate the acceptability of tryptophan residues of proteins to the solvent molecules, acrylamide-induced fluorescence quenching was studied. The intrinsic protein fluorescence was excited at 297 and recorded at 340 nm. The recorded values were corrected based on solvent signal. The quenching constant was evaluated using the Stern−Volmer equation $I_0/I = 1 + K_{sv}[Q]$, where I_0 and I are the fluorescence intensities in the absence and presence of quencher, K_{SV} is the Stern−Volmer

Table 1. Characteristics of the Intrinsic Fluorescence of GGBP and Its Mutant Forms, As Well As Their Complexes with D-Glucose, in the Native State and the Unfolded State Caused by GdnHCl

	fluorescence				quenching	
protein	λ_{max}, nm (λ_{ex} = 297 nm)	parameter A(λ_{ex} = 297 nm)	r (λ_{ex} = 297 nm, λ_{em} = 365 nm)	$\langle\tau\rangle^*$, ns (λ_{ex} = 297 nm, λ_{em} = 340 nm)	K_{sv}, M^{-1}	k_q, 10^9 M^{-1} C^{-1}
GGBP	338	1.0	0.15	7.03 ± 0.09	4.66 ± 0.07	0.66 ± 0.02
GGBP/Glc	336−337	1.0	0.16	6.96 ± 0.15	1.87 ± 0.13	0.27 ± 0.02
GGBP-W183A	332−333	1.6	0.13	4.12 ± 0.09	6.90 ± 0.36	1.68 ± 0.12
GGBP-W183A/Glc	330−331	1.7	0.14	4.04 ± 0.03	7.52 ± 0.33	1.86 ± 0.10
GGBP-F16A	339	0.94	0.13	6.93 ± 0.32	9.66 ± 0.39	1.39 ± 0.12
GGBP-F16A/Glc	338	0.95	0.15	7.14 ± 0.29	4.28 ± 0.12	0.60 ± 0.04
GGBP-F39A and GGBP-W183A in the presence of 3.0 M GdnHCl	348−349	0.47	0.06			

* The values of fluorescence life times are an average of three experiments.

quenching constant and [Q] is the quencher concentration.[30,31] The bimolecular quenching rates, k_q, have been calculated from K_{SV} and the mean-square fluorescence lifetime, τ, as $k_q = K_{SV}/\tau$ (M^{-1} s^{-1}).[30]

DSC Measurements. Differential scanning calorimetry (DSC) experiments were performed using a DASM-4 differential scanning microcalorimeter ("Biopribor", Pushchino, Russia) as described earlier.[32−35] Protein samples (0.65−0.7 mg/mL) were heated at a constant rate of 1 K/min and a constant pressure of 2.4 atm. The reversibility of the thermal transitions was assessed by reheating the sample immediately after the cooling step from the previous scan. The thermal transition curves were baseline corrected by subtracting a scan of the buffer only in both cells. The excess heat capacity of the protein (C_p) was calculated as described by Privalov and Potekhin.[36] The temperature dependence of the excess heat capacity was analyzed using Origin software (Micro-Cal Inc., Northampton, MA). The thermal stability of the proteins was described by the temperature of the maximum of thermal transition (T_m), and calorimetric enthalpy (ΔH_{cal}) was calculated as the area under the excess heat capacity curve. The thermal transition curves were further analyzed for determination of the number of two-state transitions (calorimetric domains) using the Origin software (Micro-Cal). The deconvolution procedure was previously described by Freire and Biltonen.[37] Each calorimetric domain was characterized by the ΔH_{cal} and the midpoint of thermal transition T_m.

RESULTS

Structural and Functional Features of GGBP Mutant Variants Compared to the Wild-Type Protein. Secondary and tertiary structures of GGBPwt and mutant GGBPs with substitutions W183A or F16A have been studied by intrinsic UV-fluorescence spectroscopy, far- and near-UV CD and tryptophan fluorescence quenching by acrylamide.

As it has been shown earlier, the tryptophan fluorescence spectrum (λ_{ex} = 297 nm) of GGBPwt in the native state has an emission maximum at 338 nm (Table 1, Figure 3). Ligand binding to GGBPwt (GGBPwt/Glc) leads to a small increase of the fluorescence emission intensity (Figure 3). The tryptophan fluorescence spectra of GGBP-W183A is blue-shifted (5−6 nm) with respect to that of GGBPwt. The change F16A does not influence fluorescence spectrum position (Table 1, Figure 3). Addition of glucose results in an increase of fluorescence intensity of both GGBP mutant variants. It is worth noting that the GGBP-F16A

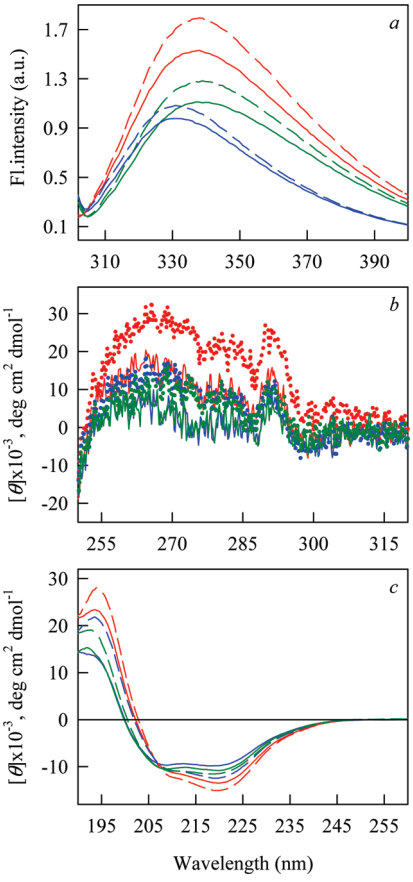

Figure 3. Influence of W183A and F16A substitutions on the tertiary and secondary structures of GGBP mutant variants as revealed by tryptophan fluorescence at 297 nm (panel a), near-UV CD (panel b), and far-UV CD (panel c). Spectra of GGBPwt (red curves), GGBP-W183A (blue curves), and GGBP-F16A (green curves) are drawn as solid lines, and spectra of these proteins in the presence of glucose are shown as dashed (panels a and c) or dotted (panels b) lines.

tryptophan fluorescence intensity is significantly lower than that of the wild-type protein, but it is higher than that of GGBP-W183A.

The tryptophan decay curves of GGBPwt and of the two mutant variants show a best fit to a three exponential model, as it is usually expected for the decay of multitryptophan proteins.

dx.doi.org/10.1021/jp204555h |J. Phys. Chem. B 2011, 115, 9022–9032

Table 2. Evaluation of the Content of Different Element of Protein Secondary Structure Based on Provencher's Analyses[38]

	portion of α-helices		portion of β-sheets		portion of β-turns		unfolded structure portion	
protein	portion	% with respect to wild type protein	portion	% with respect to wild type protein	portion	% with respect to wild type protein	portion	% with respect to wild type protein
GGBP	0.36		0.19		0.19		0.27	
GGBP (X-ray data)	0.43		0.18					
GGBP/Glc	0.40	113	0.16	87	0.18	97	0.26	95
GGBP-W183A	0.24	67	0.24	127	0.21	112	0.32	116
GGBP-W183A/Glc	0.34	94	0.19	103	0.19	103	0.28	103
GGBP-F16A	0.24	69	0.23	124	0.21	111	0.32	117
GGBP-F16A/Glc	0.30	84	0.21	114	0.20	108	0.29	106

The excited state lifetime of GGBP-W183A is significantly shorter with respect to that of GGBPwt and of GGBP-F16A, and this is likely due to the substitution of Trp183 with an alanine residue (Table 1).

Upon glucose binding the lifetime values of GGBPwt and mutant GGBPs remain practically unchanged. The value of the bimolecular constants of tryptophan fluorescence quenching by acrylamide can be used to evaluate the accessibility of tryptophan residues to solvent molecules. The values for wt GGBP and both mutants are the following: GGBPwt ($0.66 \pm 0.02 \times 10^9$ M^{-1} s^{-1}) < GGBP-F16A ($1.39 \pm 0.12 \times 10^9$ M^{-1} s^{-1}) < GGBP-W183A ($1.68 \pm 0.12 \times 10^9$ M^{-1} s^{-1}). These values are lower than the values of the bimolecular quenching constant of free tryptophan in water (5.9×10^9 M^{-1} s^{-1}), indicating a significant shielding of tryptophan residues from the solvent molecules in GGBPwt and mutant GGBPs (Table 1).

Addition of glucose leads to a decrease of the bimolecular constant value of GGBPwt ($0.27 \pm 0.02 \times 10^9$ M^{-1} s^{-1}) and GGBP-F16A ($0.60 \pm 0.04 \times 10^9$ M^{-1} s^{-1}) and an increase of the constant of GGBP-W183A ($1.86 \pm 0.02 \times 10^9$ M^{-1} s^{-1}).

Near-UV CD spectra of GGBP-W183A and GGBP-F16A are less pronounced than that of the wild-type protein but retain all of the bands observed in the GGBPwt. Upon glucose addition, an increase of the magnitude of the near-UV CD spectra of both GGBP mutants occurs (Figure 3).

The far-UV CD spectrum of GGBPwt has two negative bands at about 222 and 208 nm (Figure 3). These bands are typical of proteins with a high content of α-helical regions in their secondary structure. The far-UV CD spectrum becomes more pronounced upon glucose binding.

Far-UV CD spectra of GGBP-W183A and GGBP-F16A display the same negative bands at 222 and 208 nm although less intense than those of GGBPwt. In the presence of glucose there is an increase in the intensity of these bands (Figure 3).

To evaluate the content of secondary structure elements we have analyzed the far-UV CD spectra of the proteins by using the Provencher's algorithm.[38] The analysis has revealed about 36% of α-helices and only 19% of β-sheets for GGBPwt, which is consistent with the crystallographic data (Table 2). Glucose binding to GGBPwt is accompanied by slight increase in α-helices and a decrease in β-sheets and unstructured regions. The amount of α-helices, calculated for GGBPs W183A and F16A, drops in comparison to that of the wild-type protein, whereas the content of β-sheets and unstructured regions rises (Table 2). Glucose addition to the mutant GGBPs restores the amount of secondary structure elements to the level of the wild-type protein.

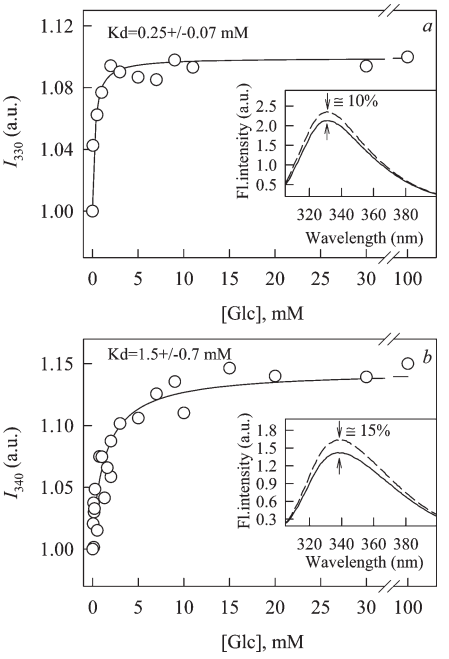

Figure 4. Determination of the dissociation constants of the complexes GGBP-W183A/Glc (panel a) and GGBP-F16A/Glc (panel b) by fluorescence intensity. A protein concentration of 0.2 mg/mL has been applied. Solid lines represent the approximation of experimental dotes under the dissociation constant determination.

A small, but clearly recorded, difference in the fluorescence intensity of mutant GGBPs in the absence and in the presence of glucose allowed us to determine the dissociation constant values of GGBP-W183A (0.28 ± 0.10 mM) and of GGBP-F16A (1.51 ± 0.88 mM) (Figure 4). These data indicate that the dissociation constants of GGBP mutant variants have been increased almost 3 orders of magnitude compared to that of GGBPwt.[13]

Conformational Changes of GGBP-W183A and GGBP-F16A Induced by GdnHCl. To characterize the stability of wild-type and mutant GGBPs, GdnHCl-induced unfolding−refolding experiments have been carried out. Different structural probes (fluorescence intensity at a fixed registration wavelength, parameter *A*, anisotropy and ellipticity at 222 nm) were used to evaluate the equilibrium dependences on GdnHCl concentration for these proteins (Figure 5). The same experiments were also performed in the presence of glucose.

dx.doi.org/10.1021/jp204555h |*J. Phys. Chem. B* 2011, 115, 9022–9032

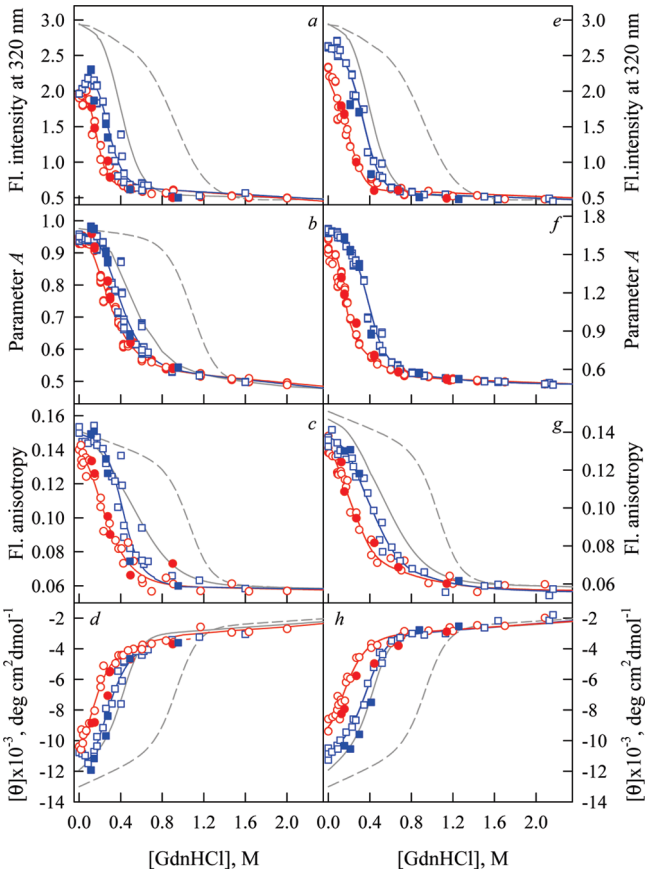

Figure 5. Conformational changes of GGBP-F16A and GGBP-F16A/Glc (red circles and blue squares, respectively; left panels) and GGBP-W183A and GGBP-W183A/Glc (red circles and blue squares, respectively; right panels) induced by GdnHCl. Fluorescent characteristic of GGBPwt (gray solid line) and GGBPwt/Glc (gray dashed line) are also shown. (a and e) Changes of the fluorescence intensity recorded at 320 nm. (b and f) Changes of parameter *A*. (c and g) Changes of fluorescence anisotropy at an excitation wavelength being equal to 297 nm. (d and h) Changes of ellipticity at 222 nm. Open symbols indicate unfolding, whereas closed symbols represent refolding of protein.

In the presence of 3.0 M GdnHCl values of parameter *A* and of the fluorescence anisotropy of the studied proteins alone and in their complexes with glucose correspond to the values showed by the completely unfolded protein (Table 1). Thus we have varied the GdnHCl concentration from 0.0 to 3.0 M.

The equilibrium dependences of the parameter *A* and of the fluorescence anisotropy on the GdnHCl concentration for GGBPwt, GGBP-W183A, and GGBP-F16A both in open and in closed forms present a sigmoid shape (Figure 5), suggesting a one-step unfolding process for GGBPwt and for the two mutants.

The equilibrium dependences of the fluorescence intensity at 320 and 365 nm and the molar ellipticity at 222 nm of GGBP-W183A and GGBP-F16A in the open form also present a sigmoid shape. While in complexes with glucose the equilibrium dependences are characterized by extremes at a low concentration of GdnHCl (at about 0.1 M). When parametrically represented, dependences of fluorescence intensities recorded at 320 and 365 nm of mutant GGBPs both in the absence and in the presence of glucose are well described by a straight line (Figure 6), thus supporting a two-state unfolding for these proteins. It is worth to note that in all cases equilibrium dependences of different structural probes recorded for

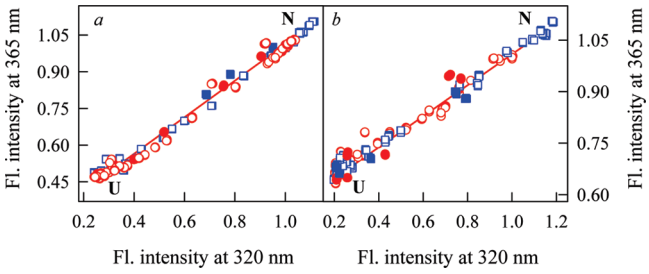

Figure 6. Parametric dependencies between the fluorescence intensities recorded at 320 and 365 nm in the unfolding processes of GGBP-F16A and GGBP-F16A/Glc (red circles and blue squares, respectively; panel a) and GGBP-W183A and GGBP-W183A/Glc (red circles and blue squares, respectively; panel b) induced by GdnHCl. The parameter is GdnHCl concentration. The excitation wavelength is 297 nm. Open symbols indicate unfolding, whereas closed symbols represent refolding. Fluorescent characteristics of the native protein state (N) and unfolded state (U) are indicated.

GGBPwt and its complexes with glucose are shifted to larger denaturant concentrations compared those of both mutant GGBPs.

The dependences of all structural probes of the studied proteins on GdnHCl concentration regarding protein unfolding and refolding coincide, implying the reversibility of the unfolding of these mutant proteins both in the absence and in the presence of glucose (Figures 5 and 6).

The difference of protein free energy between native and unfolded state (ΔG^0) has been estimated for the mutant GGBPs alone and in complexes with glucose by using the equilibrium dependences of the fluorescence intensities at 320 and 365 nm (Table 3, Figure 5).

The previously calculated ΔG^0 value for GGBPwt is almost half as great as that of GGBPwt/Glc (1.92 ± 0.90 and 3.37 ± 1.07 kcal/mol, respectively; Table 3), showing a significant stabilization of the protein structure upon glucose binding.[39,40] Instead the ΔG^0 values for GGBP-W183A and GGBP-F16A change insignificantly upon glucose binding. The values of ΔG^0 of GGBP-W183A and GGBP-W183A/Glc being equal to 2.0 ± 1.0 and 2.5 ± 0.4 kcal/mol, respectively, are close to the values calculated for GGBP-F16A and GGBP-F16A/Glc (2.2 ± 0.5 and 1.8 ± 0.4 kcal/mol, respectively, Table 3). The midpoint of GGBPwt/Glc unfolding (0.93 M GdnHCl) occurs at higher concentrations of GdnHCl compared to GGBPwt unfolding (0.36 M GdnHCl). This also supports the stabilizing effect of glucose on protein structure. For mutant GGBPs such a drastic effect is not observed. Glucose binding to GGBP-W183A and to GGBP-F16A results in a small shift of the transition midpoint from 0.27 to 0.33 M GdnHCl and from 0.17 to 0.22 M GdnHCl, respectively (Figure 5, Table 3). Apparently, this is due to a weaker binding of glucose to the ligand-binding site of the mutant proteins (Figure 4).

Heat Denaturation of Mutant GGBPs. To further characterize the protein's stability we have undertaken the investigation of heat-induced denaturation of GGBPwt and GGBP mutant variants in their free state and in the presence of glucose by differential scanning calorimetry (DSC) and by UV-fluorescence.

The calorimetric traces obtained for GGBPwt, GGBP-F16A and GGBP-W183A and their complexes with glucose are represented in figure 7. The heat-induced unfolding of all GGBP forms is shown to be reversible both in the presence and in the absence of the ligand as indicated by the almost complete reproducibility

dx.doi.org/10.1021/jp204555h |*J. Phys. Chem. B* 2011, 115, 9022–9032

Table 3. Thermodynamic Parameters of GGBP and Its Mutant Forms, As Well As Their Complexes with D-Glucose Determined on the Basis of a GdnHCl-Induced Unfolding Process

	GGBP*		GGBP-W183A		GGBP-F16A	
	protein	complex	protein	complex	protein	complex
m, kcal mol^{-1} M^{-1}	5.29 ± 1.42	3.60 ± 0.88	7.4 ± 1.6	7.7 ± 0.8	12.7 ± 1.6	8.3 ± 0.9
$D_{50\%}$, M	0.36 ± 0.10	0.93 ± 0.03	0.27 ± 0.07	0.33 ± 0.02	0.17 ± 0.02	0.22 ± 0.02
ΔG^0 (23 °C), kcal mol^{-1}	1.92 ± 0.9	3.37 ± 1.07	2.0 ± 1.0	2.5 ± 0.4	2.2 ± 0.5	1.8 ± 0.4

*Data are taken from ref 40.

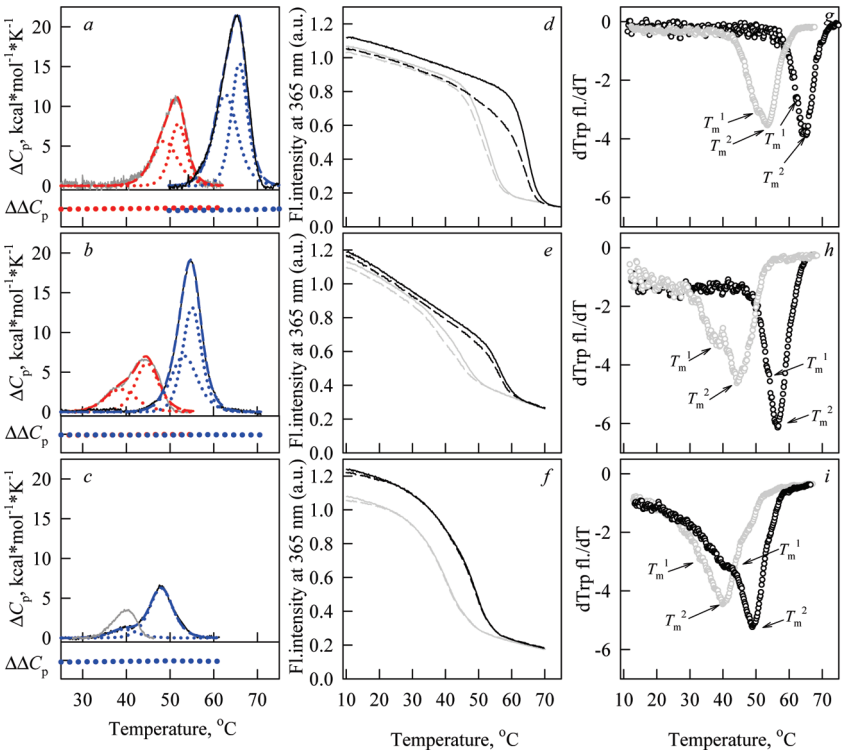

Figure 7. Heat-induced denaturation of GGBPwt and GGBPwt/Glc (gray and black lines, respectively, on panels a, d, and g), and protein mutant variants GGBP-W183A and GGBP-W183A/Glc (gray and black lines, respectively, on panel *b*, *e* and *h*), and GGBP-F16A and GGBP-F16A/Glc (gray and black lines, respectively, on panels c, f, and i) as recorded by DSC (panels a, b, and c) and fluorescence experiments (panels *d*-*i*). (panels a, b, and c) Temperature dependencies of the excess heat capacity of studied proteins. The protein concentration is 0.6−0.7 mg/mL. The deconvolution of calorimetric traces into two separate thermal transitions is shown in red for protein and in blue for the protein complex with glucose, with deviations from experimental dotes being represented in corresponding bottom panels. (panels d, e, and f) Temperature dependencies of the fluorescence intensity of studied proteins. Two sequential scans (solid and dashed lines, respectively) are shown to characterize the reversibility of the thermal transitions. (panels g, h, and i) Dependencies of the first derivative of fluorescence intensity of studied proteins are represented.

of the calorimetric traces assessed a second time by reheating the sample immediately after the cooling step (data are not shown). This is also supported by the coincidence of two sequential scans of fluorescence intensity recorded in the thermal denaturation range of these proteins alone and of their complexes with glucose (Figure 7, panels a and b). Minor deviations of repeated scans can be attributed to protein aggregation occurring at high temperature as has been previously observed for the wild-type protein.[40]

For both GGBP-W183A (T_m = 43.8 °C) and GGBP-W183A/Glc (T_m = 54.8 °C), the major thermal transition takes place at a lower temperature compared to that of the wild type protein in the absence and in the presence of the sugar (Table 4). The calorimetric enthalpy, ΔH_{cal}, of the thermal unfolding of GGBP-W183A and of GGBP-W183A/Glc is 83 and 87% of that of GGBPwt and GGBPwt/Glc, respectively. The calorimetric trace of GGBP-W183A exhibits an additional shoulder at about 38 °C. We have calculated the ratio of $\Delta H/\Delta H_{cal}$ (where ΔH, standard enthalpy change, is characterizing the width of thermal transition, see Table 5) according to van't Hoff criterion.[41] In the case of both GGBP-W183A and GGBP-W183A/Glc, this value was less than 1 indicating that the mutant protein as well as its complex with glucose unfolds only partially (Table 4). Most adequate fits of GGBP-W183A and GGBP-W183A/Glc calorimetric traces are obtained when decomposed into two individual thermal transitions (calorimetric domains, Figure 7), and summarized in table 4. The T_m values of the separate calorimetric domains of GGBP-W183A differ by more than 6 °C (Table 4), whereas the difference for GGBP-W183A/Glc is reduced to 2.5 °C.

The GGBP-F16A and GGBP-F16A/Glc are even less stable to heating in comparison to GGBP-W183A and GGBP-W183A/Glc (Table 4). The T_m of major thermal transitions revealed by

dx.doi.org/10.1021/jp204555h |J. Phys. Chem. B 2011, 115, 9022–9032

Table 4. Calorimetric Parameters Obtained from DSC Data for Thermal Transitions of GGBP and Its Mutant Forms, As Well As Their Complexes with D-Glucose[a]

protein sample	ΔH_{cal},kcal/mol	T_m, °C	$\Delta H/\Delta H_{cal}$	T_m^1, °C	ΔH^1, kcal/mol	T_m^2, °C	ΔH^2, kcal/mol
			GGBP-W183A				
protein	72	43.8	0.75	38.4	23.5	44.6	35.4
complex	119	54.8	0.95	52.7	38.4	55.2	51.8
			GGBP-F16A				
protein	23	39.5	1.95				
complex	53	47.6	0.97	39.3	12.7	48	34.4
			GGBP				
protein	87	51.3	0.99	48.8	32	51.9	37
complex	137	64.7	0.98	62	43	65.3	57

[a] The parameters were extracted from Figure 7. The errors of the given values of transition temperature (T_m) did not exceed ±0.2 °C. The relative errors of the given values of calorimetric enthalpy, ΔH_{cal}, did not exceed ±10%.

Table 5. Thermodynamic Parameters of GGBP and Its Mutant Forms, As Well As Their Complexes with D-Glucose Determined on the Basis of a Heat-Induced Unfolding Process

	GGBP-W183A		GGBP-F16A		GGBP-wt	
	protein	complex	protein	complex	protein	complex
T_m, °C	43.83 ± 0.05	56.70 ± 0.03	39.3 ± 0.1	47.6 ± 0.1	52.50 ± 0.02	64.6 ± 0.02
ΔG^0 (23 °C), kcal mol^{-1}	1.94 ± 0.01	4.15 ± 0.02	1.46 ± 0.01	1.93 ± 0.02	3.6 ± 0.01	5.30 ± 0.01
ΔH^0(23 °C), kcal · mol^{-1}	55.4 ± 0.7	112.6 ± 1.0	45.0 ± 0.3	51.2 ± 0.9	85.7 ± 0.5	134 ± 1.0
ΔC_p^0, kcal · mol^{-1} · deg^{-1}	2.44 ± 0.05	4.12 ± 0.05	2.04 ± 0.03	2.06 ± 0.05	3.03 ± 0.04	3.7 ± 0.2

calorimetric traces is 39.5 and 47.6 °C for GGBP-F16A and GGBP-F16A/Glc and are 12 and 17 °C lower than those of GGBP-wt and GGBP-wt/Glc (Table 4, Figure 7). The calorimetric trace of GGBP-F16A/Glc contains a shoulder at about 39 °C. The calorimetric trace of GGBP-F16A/Glc can be decomposed into two separate thermal transitions that are in agreement with the calculated ratio of $\Delta H/\Delta H_{cal}$ (Table 4). In contrast to that of GGBP-F16A/Glc, the calorimetric trace of GGBP-F16A does not have any visible shoulder in the proximity of the major peak (Figure 7). The ratio of $\Delta H/\Delta H_{cal}$ is close to 2 (Table 4). The protein calorimetric enthalpy of GGBP-F16A is 26% of the ΔH_{cal} of GGBPwt while the enthalpy variation of GGBP-F16A/Glc is 39% of that of GGBP-wt/Glc.

Calorimetric traces of GGBPwt and its complex with glucose have a single peak with T_m of 51.3 and 64.7 °C, respectively (Table 4, Figure 7). The peaks can be decomposed into two separate thermal transitions with close T_m values (Table 4).

The dependences of fluorescence intensity on temperature of GGBPwt and mutant GGBPs, as well as their complexes with glucose, are S-shaped (Figure 7). The calculated T_m values correspond to T_m values of the main calorimetric transition (Table 4, 5). At the same time, the first derivative of fluorescence intensity of all the proteins under investigation has a complex character. The first derivative of fluorescence intensity of GGBP-W183A has two clearly distinguishable minima at temperatures corresponding to the T_m of the calorimetric domains revealed from DSC data (Table 4, Figure 7). The dependence of the first derivative of GGBP-W183A/Glc fluorescence intensity is characterized by a main minimum at 56.7 °C and a shoulder at slightly lower temperature. The existence of two thermal transitions for GGBP-F16A/Glc melting is indicated by the two minima of the first derivative of the fluorescence intensity spectra for GGBP-F16A/Glc (Figure 7). In addition to the global minima at 40 °C, small disturbances of the first derivative of fluorescence intensity of GGBP-F16A appear at 33 °C (Figure 7).

Discussion. Any change in the primary structure of a protein can abolish the proper folding into a unique structure and/or its functional activity. To elaborate GGBP variants with low affinity to Glc, we manipulated the amino acid residues located in the active center of the protein.

The substitution of Trp 183 or Phe 16 residues, which are directly involved in sugar binding in the protein active center, changes the physical-chemical properties of mutant GGBPs.

The observed difference between GGBP-W183A and GGBPwt as well as the GGBP-F16A fluorescent characteristics (fluorescence intensity and lifetime) and bimolecular quenching constant can be mainly attributed to the absence of the Trp residue responsible for the fluorescent properties of GGBP-W183A.

In general, the reduced fluorescence intensities and the less pronounced near-UV CD spectra of both mutant GGBPs indicate a loosening of GGBP tertiary structure (Figure 3). An increased accessibility of tryptophan residues of GGBP-W183A and GGBP-F16A, as revealed by the value of bimolecular quenching constant (Table 1), confirm this assumption. A presence of all characteristic bands in near-UV CD spectra of mutant GGBPs shows that the overall tertiary structure of these proteins is similar to that of the wild-type protein.

The substitution of Trp 183 or Phe 16 residues to alanine also affects the secondary structure of GGBP (Table 2, Figure 3). Any of these substitutions results in a decrease of α-helices content and an increase of β-sheets and unstructured regions compared to the wild-type protein. It is important to emphasize that protein secondary structure content is more altered by the introduction of W183A substitution into GGBP active center (see Table 2).

All recorded data imply that in the presence of glucose the tertiary structure of GGBP-W183A and GGBP-F16A become more compact and similar to that of the wild-type protein. In addition, the secondary structure elements of the mutant GGBPs are restores to a level of GGBPwt (Tables 1 and 2, Figure 3). These data also allow us to hypothesize that both mutant GGBPs preserve the ability to bind glucose. The dependences of fluorescence intensity of GGBP-W183A and GGBP-F16A on Glc concentration (Figure 4) show that the dissociation constants of these mutant proteins are in the millimolar range.

The GGBP-W183A and GGBP-F16A unfolding induced by GdnHCl seems to be a one-step reversible process (Figures 5, 6). The extreme observed on equilibrium dependencies of fluorescence intensities and far-UV CD of GGBP-W183A/Glc and GGBP-F16A/Glc can be explained by the so-called stabilizing effect of GdnHCl.[26,42] At low concentrations of GdnHCl, the $GdnH^+$ ions interact with the carboxyl groups on protein surface, resulting in neutralization of the negatively charged proteins regions. This reduces local structural tensions of protein globule and leads to some ordering of protein structure. Acting as denaturing agent at elevating concentrations GdnHCl causes protein unfolding. Decreasing of midpoint of GdnHCl-induced unfolding of mutant GGBPs reflects a destabilizing action of W183A or F16A substitutions on the whole protein structure (Table 3, Figure 5). At the same time, the structure of GGBP-W183A is more stable compared to that of GGBP-F16A.

The thermal unfolding of mutant GGBPs takes place at lower temperature with respect to the wild-type protein: GGBP-F16A being even less stable than GGBP-W183A (Table 4, Figure 6). The clearly distinguishable shoulder of the calorimetric trace of GGBP-W183A testifies a more complex character of protein unfolding than it has been shown by GdnHCl-induced denaturation of the protein. As GGBP has a two-domains structure, the behavior of the calorimetric trace of GGBP-W183A can be attributed to the separate protein domains that possess a different thermal stability. This is proved by comparison the changes of enthalpy determined by calorimetry and by experiments on the protein intrinsic fluorescence. As it is predicted the value of $\Delta H/\Delta H_{cal}$ ratio is less than 1 (Table 4). It means that the mutant protein melts partially.

In the case of the complex GGBP-W183A/Glc, the value of $\Delta H/\Delta H_{cal}$ is close to unity, though deconvolution of calorimetric traces of GGBP-W183A/Glc can be presented by two individual thermal transitions. The 6 °C difference of T_m values of two domains of GGBP-W183A shows a noncooperative protein melting process (Table 4). The glucose binding to GGBP-W183A results in an increase of thermal stability of the protein domains as indicated by the increase of T_m of the protein individual domains and by the reduction of T_m difference to 2.5 °C. Obviously, the presence of glucose in the structure of GGBP-W183A makes the thermal unfolding of the two protein domains strictly bounded, thus increasing protein thermo-stability (more than 10 °C).

Calculated from the temperature dependences of fluorescence intensity of GGBP-W183A and GGBP-W183A/Glc the T_m values correspond to the T_m values of the main calorimetric transition of the mutant protein and its complex with glucose (Tables 4, 5). Since only one of the four tryptophan residues of GGBP (Trp 284) is located at the N-terminal domain whereas all the others (Trp 127, Trp 133, and Trp 195) are located at the protein C-terminal domain[39,43] (Trp 183 of wild-type protein is eliminated from the structure of GGBP-W183A) it seems that fluorescence data reflect the thermal stability of the protein C-terminal domain. Thus the high-temperature transition corresponds to thermal unfolding of C-terminal domain of GGBP-W183A and GGBP-W183A/Glc. Meanwhile, the character of the first derivative of fluorescence intensity of GGBP-W183A and GGBP-W183A/Glc reveals the existence of the both thermal transitions as monitored by DSC (Table 4, Figure 7). Taken together, all experimental data show that the N-terminal domain of GGBP-W183A possesses an appreciably lower thermo-stability compared to C-terminal domain. The increased protein stability and the recovery of the cooperativity during the thermal unfolding process of the complex GGBP-W183A/Glc arise from a tightly bounded melting of separate domains of protein in the presence of glucose.

Experimental data shows that GGBP-F16A/Glc also melts partially with the C-terminal domain being more stable compared to N-terminal protein domain (Table 4, Figure 7), though the peak of thermal flux is rather small in comparison with GGBPwt and GGBP-W183A/Glc. This suggests a low cooperativity during the process of melting as well as high error in ΔH_{cal} evaluation.[44] The determination of ΔH is also of high inaccuracy. So in this case the ratio of $\Delta H/\Delta H_{cal}$ does not allow making valid conclusions about the succession of the protein domain melting.

The existence of noncooperative melting transitions has been earlier described for several proteins.[45,46] The assumption that part of GGBP-F16A unfolds noncooperatively is corroborated by under-evaluated value of protein calorimetric enthalpy (it is equal to 26% of ΔH_{cal} of GGBPwt as compared to 39% of ΔH_{cal} of GGBP-wt/Glc for GGBP-F16A/Glc) and by the slightly distinguishable shoulder at 33 °C in the first derivative of the fluorescence intensity spectrum of GGBP-F16A which appeared in addition to the global minima at 40 °C (Table 4, Figure 7). Close thermal characteristics of separate protein domains of GGBPwt and its complex with glucose revealed by DSC data (Table 4) imply that N- and C-terminal domains of wild-type protein have similar thermal stability indicating that the thermal unfolding of GGBPwt is a one-step process. In conclusion, the substitution of Trp183 in GGBP results in the decrease of the thermostability of the both protein domains. The binding of glucose to GGBP-W183A restores the stability of domains and shift the cooperativity of the protein unfolding to a large degree.

The effect of Phe 16 substitution on the thermal stability of the entire GGBP structure is very pronounced: GGBP-F16A possesses a low stability even when it is in complex with the ligand. These data imply that Phe 16 is crucial for the protein stability.

Summarizing all of the experimental data we can conclude that GGBP-W183A is a promising mutant form of GGBP for use as a sensing probe in a biosensor system designed to detect glucose in the blood.

Though W183A substitution results in a drastic increase of protein−ligand dissociation constant, further fine-tuning of sensitivity of the protein to glucose concentration can be achieved by additional substitutions of residues that could donate hydrogen bonds to glucose molecule directly or via other residues. These manipulations should be accomplished carefully as, for example, substitution of Asn 256 can abolished glucose binding.[47] In fact, it has been shown that Asn 256 is highly conserved residue among glucose-binding proteins from different prokaryotic organisms.

AUTHOR INFORMATION

Corresponding Authors

*(K.K.T.) Tel.: 7(812) 2971957. Fax: 7(812) 2970341. E-mail: kkt@mail.cytspb.rssi.ru. (S.D.) Tel.: +39-0816132250. Fax: +39-0816132277. E-mail: s.dauria@ibp.cnr.it.

■ ACKNOWLEDGMENT

This work was in parts supported by Ministry of Education and Science (Contracts 02.740.11.5141, P1198, and 16.512.11.2114), Program MCB RAS and grants from the president of RF (MK-1181.2010.4), and by the Program CNR-RAS 2011-2013 (S.D., M.S., K.K.T., and I.K.), and CNR Commessa in Agro Food (S.D. and M.S.). We thank Dr. Paolo Bazzicalupo for language revision of the manuscript.

■ ABBREVIATIONS:

CD, circular dichroism DASM, differential adiabatic scanning microcalorimetry GGBPwt, wild-type of D-glucose/D-galactose binding protein GGBP-F16A and GGBP-W183A, GGBP with Phe16Ala and Trp183Ala substitutions, respectively GGBPwt/Glc, GGBP-F16A/Glc, GGBP-W183A/Glc, a complexes of wild-type protein and GGBP mutant variants with glucose GdnHCl, guanidine hydrochloride IPTG, isopropyl-beta-D-1-thiogalactopyranoside UV, ultraviolet

■ REFERENCES

(1) Oliver, N. S.; Toumazou, C.; Cass, A. E.; Johnston, D. G. Glucose sensors: a review of current and emerging technology. *Diabet Med.* **2009**, *26* (3), 197–210.

(2) Shaw, J. E.; Sicree, R. A.; Zimmet, P. Z. Global estimates of the prevalence of diabetes for 2010 and 2030. *Diabetes Res. Clin. Pract.* **2010**, *87* (1), 4–14.

(3) Wojcicki, J. M.; Ladyzynski, P. Toward the improvement of diabetes treatment: recent developments in technical support. *J. Artif. Organs* **2003**, *6* (2), 73–87.

(4) Ferrante do Amaral, C. E.; Wolf, B. Current development in non-invasive glucose monitoring. *Med. Eng. Phys.* **2008**, *30* (5), 541–9.

(5) Ervin, K. R.; Kiser, E. J. Issues and implications in the selection of blood glucose monitoring technologies. *Diabetes Technol. Ther.* **1999**, *1* (1), 3–11.

(6) Tura, A.; Maran, A.; Pacini, G. Non-invasive glucose monitoring: assessment of technologies and devices according to quantitative criteria. *Diabetes Res. Clin. Pract.* **2007**, *77* (1), 16–40.

(7) Moschou, E. A.; Sharma, B. V.; Deo, S. K.; Daunert, S. Fluorescence glucose detection: advances toward the ideal in vivo biosensor. *J. Fluoresc.* **2004**, *14* (5), 535–47.

(8) Tolosa, L. On the design of low-cost fluorescent protein biosensors. *Adv. Biochem. Eng. Biotechnol.* **2009**, *116*, 143–57.

(9) Shilton, B. H.; Flocco, M. M.; Nilsson, M.; Mowbray, S. L. Conformational changes of three periplasmic receptors for bacterial chemotaxis and transport: the maltose-, glucose/galactose- and ribose-binding proteins. *J. Mol. Biol.* **1996**, *264* (2), 350–63.

(10) Tam, R.; Saier, M. H., Jr. Structural, functional, and evolutionary relationships among extracellular solute-binding receptors of bacteria. *Microbiol. Rev.* **1993**, *57* (2), 320–46.

(11) Dwyer, M. A.; Hellinga, H. W. Periplasmic binding proteins: a versatile superfamily for protein engineering. *Curr. Opin. Struct. Biol.* **2004**, *14* (4), 495–504.

(12) Borrok, M. J.; Kiessling, L. L.; Forest, K. T. Conformational changes of glucose/galactose-binding protein illuminated by open, unliganded, and ultra-high-resolution ligand-bound structures. *Protein Sci.* **2007**, *16* (6), 1032–41.

(13) Vyas, N. K.; Vyas, M. N.; Quiocho, F. A. Sugar and signal-transducer binding sites of the Escherichia coli galactose chemoreceptor protein. *Science* **1988**, *242* (4883), 1290–5.

(14) Vyas, N. K.; Vyas, M. N.; Quiocho, F. A. Comparison of the periplasmic receptors for L-arabinose, D-glucose/D-galactose, and D-ribose. Structural and Functional Similarity. *J. Biol. Chem.* **1991**, *266* (8), 5226–37.

(15) Vyas, M. N.; Vyas, N. K.; Quiocho, F. A. Crystallographic analysis of the epimeric and anomeric specificity of the periplasmic transport/chemosensory protein receptor for D-glucose and D-galactose. *Biochemistry* **1994**, *33* (16), 4762–8.

(16) Tolosa, L.; Gryczynski, I.; Eichhorn, L. R.; Dattelbaum, J. D.; Castellano, F. N.; Rao, G.; Lakowicz, J. R. Glucose sensor for low-cost lifetime-based sensing using a genetically engineered protein. *Anal. Biochem.* **1999**, *267* (1), 114–20.

(17) Renard, E. Monitoring glycemic control: the importance of self-monitoring of blood glucose. *Am. J. Med.* **2005**, *118* (Suppl 9A), 12S–19S.

(18) Turoverov, K. K.; Kuznetsova, I. M.; Uversky, V. N. The protein kingdom extended: ordered and intrinsically disordered proteins, their folding, supramolecular complex formation, and aggregation. *Prog. Biophys. Mol. Biol.* **2010**, *102* (2−3), 73–84.

(19) Harayama, S.; Bollinger, J.; Iino, T.; Hazelbauer, G. L. Characterization of the mgl operon of Escherichia coli by transposon mutagenesis and molecular cloning. *J. Bacteriol.* **1983**, *153* (1), 408–15.

(20) Rotman, B.; Ganesan, A. K.; Guzman, R. Transport systems for galactose and galactosides in Escherichia coli. II. Substrate and inducer specificities. *J. Mol. Biol.* **1968**, *36* (2), 247–60.

(21) Laemmli, U. K. Cleavage of structural proteins during the assembly of the head of bacteriophage T4. *Nature* **1970**, *227* (5259), 680–5.

(22) Turoverov, K. K.; Biktashev, A. G.; Dorofeiuk, A. V.; Kuznetsova, I. M. [A complex of apparatus and programs for the measurement of spectral, polarization and kinetic characteristics of fluorescence in solution]. *Tsitologiia* **1998**, *40* (8−9), 806–17.

(23) Turoverov, K. K.; Kuznetsova, I. M. Intrinsic fluorescence of actin. *J. Fluoresc.* **2003**, *13*, 41–57.

(24) Eftink, M. R. The use of fluorescence methods to monitor unfolding transitions in proteins. *Biophys. J.* **1994**, *66* (2 Pt 1), 482–501.

(25) Kuznetsova, I. M.; Stepanenko, O. V.; Stepanenko, O. V.; Povarova, O. I.; Biktashev, A. G.; Verkhusha, V. V.; Shavlovsky, M. M.; Turoverov, K. K. The place of inactivated actin and its kinetic predecessor in actin folding-unfolding. *Biochemistry* **2002**, *41* (44), 13127–32.

(26) Kuznetsova, I. M.; Stepanenko, O. V.; Turoverov, K. K.; Zhu, L.; Zhou, J. M.; Fink, A. L.; Uversky, V. N. Unraveling multistate unfolding of rabbit muscle creatine kinase. *Biochim. Biophys. Acta* **2002**, *1596* (1), 138–55.

(27) Kuznetsova, I. M.; Turoverov, K. K.; Uversky, V. N. Use of the phase diagram method to analyze the protein unfolding-refolding reactions: fishing out the "invisible" intermediates. *J. Proteome Res.* **2004**, *3* (3), 485–94.

(28) Stepanenko, O. V.; Kuznetsova, I. M.; Turoverov, K. K.; Huang, C.; Wang, C. C. Conformational change of the dimeric DsbC molecule induced by GdnHCl. A study by intrinsic fluorescence. *Biochemistry* **2004**, *43* (18), 5296–303.

(29) Nolting, B., *Protein Folding Kinetics. Biophysical Methods*; Springer-Verlag: Berlin, 1999; p 191.

(30) Eftink, M. R. Fluorescence techniques for studying protein structure. *Methods Biochem. Anal.* **1991**, *35*, 127–205.

(31) Staiano, M.; D'Auria, S.; Varriale, A.; Rossi, M.; Marabotti, A.; Fini, C.; Stepanenko, O. V.; Kuznetsova, I. M.; Turoverov, K. K. Stability and dynamics of the porcine odorant-binding protein. *Biochemistry* **2007**, *46* (39), 11120–7.

(32) Kremneva, E.; Boussouf, S.; Nikolaeva, O.; Maytum, R.; Geeves, M. A.; Levitsky, D. I.; Levitsky, D. I.; Rostkova, E. V.; Orlov, V. N.; Nikolaeva, O. P.; Moiseeva, L. N.; Teplova, M. V.; Gusev, N. B. Effects of two familial hypertrophic cardiomyopathy mutations in alpha-tropomyosin, Asp175Asn and Glu180Gly, on the thermal unfolding of actin-bound tropomyosin. *Biophys. J.* **2004**, *87* (6), 3922–33.

(33) Levitsky, D. I.; Rostkova, E. V.; Orlov, V. N.; Nikolaeva, O. P.; Moiseeva, L. N.; Teplova, M. V.; Gusev, N. B. Complexes of smooth muscle tropomyosin with F-actin studied by differential scanning calorimetry. *Eur. J. Biochem.* **2000**, *267* (6), 1869–77.

(34) Levitsky, D. I., *Structural and functional studies of muscle proteins by using differential scanning calorimetry*; Kluwer Academic Publishers: Dordrecht, The Netherlands, 2004; pp 127−158.

(35) Markov, D. I.; Pivovarova, A. V.; Chernik, I. S.; Gusev, N. B.; Levitsky, D. I. Small heat shock protein Hsp27 protects myosin S1 from

heat-induced aggregation, but not from thermal denaturation and ATPase inactivation. *FEBS Lett.* **2008**, *582* (10), 1407–12.

(36) Privalov, P. L.; Potekhin, S. A. Scanning microcalorimetry in studying temperature-induced changes in proteins. *Methods Enzymol.* **1986**, *131*, 4–51.

(37) Freire, E.; Biltonen, R. L. Statistical mechanical deconvolution of thermal transitions in macromolecules. I. Theory and application to homogeneous systems. *Biopolymers* **1978**, *17*, 463–479.

(38) Provencher, S. W.; Glockner, J. Estimation of globular protein secondary structure from circular dichroism. *Biochemistry* **1981**, *20* (1), 33–7.

(39) Stepanenko, O. V.; Povarova, O. I.; Stepanenko, O. V.; Fonin, A. V.; Kuznetsova, I. M.; Turoverov, K. K.; Staiano, M.; D'Auria, S. Structure and stability of D-galactose/D-glucose-binding protein. The role of D-glucose binding and Ca ion depletion. *Spectrosc. Biomed. Appl.* **2009**, *24* (3−4), 355–359.

(40) Stepanenko, O. V.; Stepanenko, O. V.; Povarova, O. I.; Fonin, A. V.; Kuznetsova, I. M.; Turoverov, K. K.; Staiano, M.; Varriale, A.; D'Auria, S. New Insight into Protein-Ligand Interactions. The Case of the d-Galactose/d-Glucose-Binding Protein from Escherichia coli. *J. Phys. Chem. B* **2011**, *115* (12), 2765–73.

(41) Finkel'shtein, A. V.; Ptitsyn, O. B. *Protein physics*; Book house "University": Moskow, 2002; p 376.

(42) Bushmarina, N. A.; Kuznetsova, I. M.; Biktashev, A. G.; Turoverov, K. K.; Uversky, V. N. Partially folded conformations in the folding pathway of bovine carbonic anhydrase II: a fluorescence spectroscopic analysis. *ChemBioChem* **2001**, *2* (11), 813–21.

(43) Scognamiglio, V.; Scire, A.; Aurilia, V.; Staiano, M.; Crescenzo, R.; Palmucci, C.; Bertoli, E.; Rossi, M.; Tanfani, F.; D'Auria, S. A strategic fluorescence labelling of D-galactose/D-glucose-binding protein from E. coli helps to shed light on the protein structural stability and dynamics. *J. Proteome Res.* **2007**, *6* (11), 4119–4126.

(44) Kremneva, E.; Nikolaeva, O.; Maytum, R.; Arutyunyan, A. M.; Kleimenov, S. Y.; Geeves, M. A.; Levitsky, D. I. Thermal unfolding of smooth muscle and nonmuscle tropomyosin alpha-homodimers with alternatively spliced exons. *FEBS J.* **2006**, *273* (3), 588–600.

(45) Kremneva, E. V.; Nikolaeva, O. P.; Gusev, N. B.; Levitsky, D. I. Effects of troponin on thermal unfolding of actin-bound tropomyosin. *Biochemistry (Mosc.)* **2003**, *68* (7), 802–9.

(46) Bogatcheva, N. V.; Gusev, N. B. Interaction of smooth muscle calponin with phospholipids. *FEBS Lett.* **1995**, *371* (2), 123–6.

(47) Amiss, T. J.; Sherman, D. B.; Nycz, C. M.; Andaluz, S. A.; Pitner, J. B. Engineering and rapid selection of a low-affinity glucose/galactose-binding protein for a glucose biosensor. *Protein Sci.* **2007**, *16* (11), 2350–9.

(48) Dutta, S.; Burkhardt, K.; Young, J.; Swaminathan, G. J.; Matsuura, T.; Henrick, K.; Nakamura, H.; Berman, H. M. Data deposition and annotation at the worldwide protein data bank. *Mol. Biotechnol.* **2009**, *42* (1), 1–13.

(49) Hsin, J.; Arkhipov, A.; Yin, Y.; Stone, J. E.; Schulten, K. Using VMD: an introductory tutorial. *Current Protocols in Bioinformatics*; Wiley: New York, 2008; Chapter 5, Unit 5 7.

(50) Merritt, E. A.; Bacon, D. J. Raster3D: Photorealistic molecular graphics. *Methods Enzymol.* **1977**, *277*, 505–524.